Supplementary Material (ESI) for Lab on a Chip


**Supplementary Material for**

# Controlled encapsulation of single cells into monodisperse picoliter drops

Jon F. Edd*, Dino Di Carlo*, Katherine J. Humphry, Sarah Köster,

Daniel Irimia, David A. Weitz & Mehmet Toner

* These authors contributed equally to this work.

**Table of Contents**

# Supplementary Materials and Methods

**Materials.** Fluorescent polystyrene microparticles (density ~ 1.05 g/mL, 9.9 μm diameter, product #G1000) were purchased from Duke Scientific (Fremont, CA). Particles were mixed to desired weight fractions by dilution in Phosphate buffered saline (PBS) and stabilized by addition of 0.1 % w/v Tween 20 (Sigma-Aldrich, St. Louis, MO). Cells (HL60 human promyelocytic leukemia cells, #CCL-240; ATCC, Manassas, VA) were cultured in RPMI 1640 medium with 10% FBS and resuspended in PBS prior to use. A live-dead assay based on calcein AM and ethidium homodimer-2 (Invitrogen, Carlsbad, CA) was used to determine cell viability / membrane integrity according to established protocols.

For beads, we used FC-40 (3M, St. Paul, MN) with oil-phase surfactant courtesy of RainDance Technologies (Lexington, MA) who also provided the fluorinated oil and PFPE-PEG block copolymer surfactant mixture (1.8 % w/w in oil) we used in the cell experiments. We also added 0.1 % w/w Zonyl FSN-100 (DuPont, Wilmington, DE) to the aqueous phase for cell experiments to reduce biological interactions with the oil-water interface.

**Microfabrication.** Devices were fabricated using soft lithography techniques. SU-8 50 (MicroChem, Newton, MA) was spun at 2400 rpm for 30 seconds to create a 52 μm thick layer on a 10 cm silicon wafer. Thickness was measured using a Dektak profilometer. The pattern was photolithographically defined in this layer using a mylar mask printed at 50,000 dpi. After development, PDMS (Sylgard 184; Dow Corning, Midland, MI) was poured onto the SU-8 master at a 10:1 ratio of base to crosslinker, degassed in a vacuum chamber, and cured at 65 °C overnight. The devices were then cut from the mold; ports were subsequently punched with a sharpened flat tip needle and devices were bonded to glass slides using oxygen plasma. After plasma treatment and placement onto the glass substrate the devices were kept at 70 °C

on a hotplate for 15 minutes to increase bonding. To ensure hydrophobic surfaces throughout the microchannels, and thus allow the oil to preferentially wet the channel walls, we manually forced the contents of a 1 mL syringe, filled with air and a small amount of Aquapel (PPG Industries, Pittsburgh, PA) inside the needle, through the channel network until no residue was visible. Channel width was measured optically during operational conditions.

**Experimental Setup.** Bead or cell suspensions and oil were separately introduced into two syringes and connected by either PEEK tubing (#1569; Upchurch Scientific, Oak Harbor, WA) or Tygon tubing (TGY-010; Small Parts) to the two inlets of the PDMS portion of the device. Outlets of PEEK tubing were also connected to the outlet ports of the device and routed into a waste container or collection tube.

Flow was driven at constant volume rate by a syringe pump (PHD 2000; Harvard Apparatus, Holliston, MA). A glass syringe (1 mL; SGE, Austin, TX) with an inserted magnetic stir bar was utilized to maintain well suspended solutions of particles prior to their injection, through a mechanism based on that reported recently where a steel ball bearing is moved magnetically within the syringe to induce mixing (R. Cooper and L. P. Lee, “Chips & Tips: Preventing suspension settling during injection,” *Lab on a Chip*, 21 August 2007). We used a plastic syringe (1 mL; BD, Franklin Lakes, NJ) to drive oil with a flow rate of 50-60 μL/min for bead experiments and 85 μL/min for cell experiments. The aqueous flow was set to 10 μL/min for beads and 13 μL/min for cells. If precautions were not taken, clogging would be a certainty as the entire suspension of particles funnels through one tiny orifice, the nozzle. We take a simple solution in the incorporation of a microfluidic filter upstream of the focusing channel, at the site of the aqueous inlet. The microfluidic filter we use is quite simple. We have included a series of narrow channels, slightly smaller in width than the narrowest point in the device, and they are arranged in a parallel fashion. Therefore, anything that enters the device that could

clog the narrow nozzle region will be caught in the filter that immediately precedes the long focusing channel, thus preventing the device from clogging catastrophically. We use a 0.2 μm PTFE syringe filter (09-720-7; Fisher Scientific, Pittsburgh, PA) for the oil inlet.

PDMS devices were mounted onto the stage of an inverted microscope (Nikon TE2000-U). High-speed camera imaging was conducted using white light in Köhler illumination with the focal plane. All neutral density filters were removed and the highest power on the lamp allowed imaging with 2 μs exposures using a Phantom v4.2 camera (Vision Research, Wayne, NJ). Frame intervals from 62.5 μs – 100 ms were used.

# Supplementary Discussion

**Particle size effects.** Although we did not explore the effect in depth, it appears that particle size (at least over the range of cell diameters) had a minor role in cross-stream ordering behavior. Inertial lift forces that lead to focusing of particles in the lateral dimension of the channel are known to scale strongly with particle size, such that for the tested system cells and particles with diameters below ~ 4 μm were seen to have less robust ordering. For larger particles, the limitation is based on the minimum channel dimension ~ 27 μm. Generation of ordered streams for particles above and below these limits (e.g. bacteria and plant cells) is expected to be possible by changing the channel dimensions appropriately. Limitations could arise for scaling to smaller dimensions as the pressure drop per unit channel length in the absence of particles is approximately equal to $32\mu\overline{V}\left(\frac{w+h}{2wh}\right)^2$, where $\mu$ is dynamic viscosity, $\overline{V}$ is the average fluid velocity and *w* and *h* are the channel width and height respectively.

**Effect of particle charge.** One can rule out an effect of surface charge in longitudinal ordering behavior based on an argument of charge screening in aqueous fluids. Water acts very much like a conductor when ionic species are dissolved within it and these charged particles within solution are associated with an electric field that decays very rapidly with distance from the charges surface. The decay length is related to the ionic strength of the fluid and characterized by a parameter (Debye length, $\kappa^{-1}$) where: $\kappa^{-1} = \sqrt{\frac{\varepsilon RT}{2F^2 C_0}}$. Here $\varepsilon$ is the permittivity of the fluid, $R$ is the gas constant, $T$ is the absolute temperature, $F$ is Faraday's constant, and $C_0$ is the molar concentration of electrolyte. For our experiments with cells in media the molar

concentration of ~150 mM yields a Debye length of ~25 nm, three orders of magnitude shorter than the distances over which we observe particle separation (10-20 μm).

**Rate of drop generation.** For the current system we are operating at some of the fastest possible drop generation rates (~15kHz). We operate at this rate because the ordering phenomenon functions more robustly at higher channel velocities. We are limited in going above this rate much further without changes in channel geometry due to a transition from the drop-dripping to jetting behavior. This transition, as previously reported (Utada et al, *Phys. Rev. Lett.* **99,** 094502 (2007)), is dependent on the capillary number of the outer pinching flow ($C_{out} = \eta_{out} u_{out} / \gamma$) and the Weber number for the inner flow ($W_{in} = \rho_{in} d_{tip} u_{in}^2 / \gamma$). Here, $\rho$ is the density of the fluid, $\eta$ is the viscosity, $\gamma$ is the surface tension between the two phases, $d_{tip}$ is the diameter of the forming drop, and $u$ is the fluid velocity. Both dimensionless numbers should be below *O(1)* to be certain of stable dripping behavior. In our current system, further increases in drop generation rates could be achieved by tuning these parameters (e.g. by reducing surfactant concentrations to increase surface tension). Decreasing the viscosity of the outer flow could also yield dripping behavior at drop generation rates exceeding 15 kHz.

# Supplementary Video Captions

**Supplementary Video 1.** Ordered particle encapsulation. This video shows sequential high-speed images of particle encapsulation in aqueous droplets. Random arrangements of particles enter the inlet of the system and after traversing the ordering channel arrive at the droplet generator portion of the microfluidic system well ordered. The oil flow rate was tuned to match the frequency of drop generation with that of the ordering. The channel is 27 μm wide and particles are 10 μm in diameter. The video is slowed down by 1000 times (1 s = 1 ms).

**Supplementary Video 2.** Ordered cell encapsulation. This video shows sequential high-speed images of HL60 cell encapsulation in aqueous droplets. Random arrangements of cells enter the inlet of the system and after traversing the ordering channel arrive at the droplet generator portion of the microfluidic system well ordered. The oil flow rate was tuned to match the frequency of drop generation with that of the ordering. The channel is 27 μm in width and cells are ~12-18 μm in diameter. The video is slowed down by 1000 times (1 s = 1 ms).

# Supplementary Figure 1

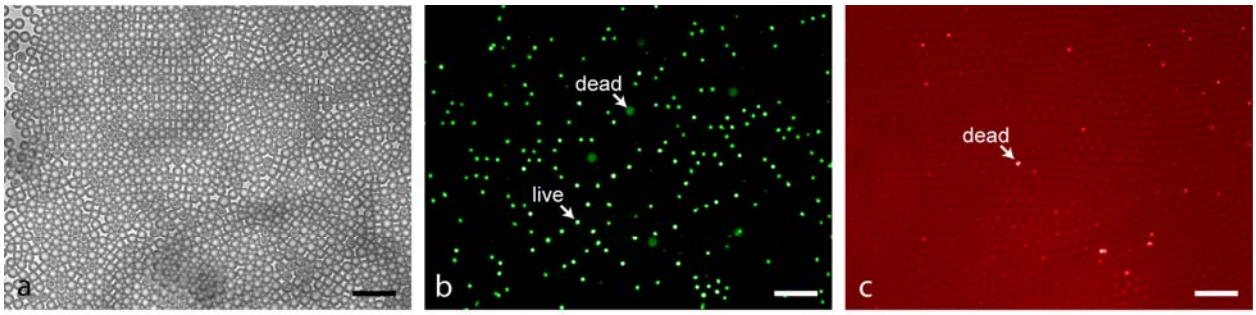


Supplementary Figure 1

**Supplementary Figure 1.** Live-dead assay for encapsulated cells. Encapsulated cells were collected and flowed into a wide microfluidic chamber. Images of cells in the largely uniform emulsion are shown in bright field (**a**), green fluorescence (**b**), and red fluorescence (**c**). Exposure time was 500 ms for green fluorescence and 10 sec for red fluorescence. Cells were stained with a live/dead stain prior to encapsulation in the system. Cells that lost membrane integrity during the cell preparation process prior to entering the chip appear bright red (**c**), while cells with membranes disrupted during the single-cell encapsulation process leak green viability dye throughout the drop in which they were encapsulated (**b**). Live cells have higher intensity green signals (**b**) that did not spread throughout the drop in question. Scale bars: 100 μm.